# Compensating XPM using a Low-Bandwidth Phase Modulator

Benjamin Foo, *Student Member, IEEE,* Bill Corcoran, *Member, IEEE,* and Arthur Lowery, *Fellow, IEEE*

***Abstract*—We experimentally demonstrate, for the first time, cross-phase modulation (XPM) compensation using an optical phase modulator and low-bandwidth electronics. We first show that our nonlinearity compensator suppresses the XPM distortion from a 10-Gbit/s on-off keyed (OOK) channel on a continuous wave (CW) probe signal. We then replace the CW tone with a 28-Gbaud quadrature phase-shift keyed (QPSK) signal and show that the OOK power can be doubled when XPM compensation is used. This demonstrates proof-of-concept for XPM compensation using phase modulators placed along a fiber link.**

***Index Terms*—Optical fiber communication, Optoelectronic devices, Phase modulation**

## I. Introduction

OPTICAL communication links are impaired by fiber nonlinearity, which limits their capacity [1]–[3]. The nonlinear distortion can be mitigated with nonlinearity compensation (NLC), though suppressing cross-phase modulation (XPM) continues to present a challenge. As XPM is the distortion of a wavelength division multiplexed (WDM) channel due to the overall intensity fluctuations of its neighbors [4], broadband NLC techniques, such as total-field digital back-propagation (TF-DBP) [5], [6] and optical phase conjugation (OPC) [7], [8], have been proposed. TF-DBP compensates the deterministic channel impairments, including XPM, at either the transmitter or receiver by digitally propagating the entire optical signal through a virtual model of the link. While TF-DBP is an extremely effective method of NLC, its implementation requires significant computational and electronic resources [6], [9]. In contrast, OPC utilizes nonlinear mixing to perform phase conjugation at one [7] or more points along a link [10], [11]. As the nonlinear distortions on a signal and on its phase conjugate cancel out, the received signal is distortion-free. However, generating the phase-conjugate necessitates high pump powers, and accurate NLC requires the link to exhibit power and dispersion symmetry [12].

A potentially simpler method to compensate XPM is to drive a phase modulator (PM) with the total power in a band of WDM channels [13], [14]. The block diagram of this technique, called a total-intensity-directed phase modulator (TID-PM) [15], is shown in Fig. 1. An optical coupler taps-off part of the WDM signal, and its total power is measured with a photodiode. The detected signal is then amplified, and used to drive a PM to suppress the nonlinear distortion. A similar technique was demonstrated in [16] to mitigate self-phase modulation. While TID-PMs would appear to require high-bandwidth photodiodes to capture the beating between widely spaced WDM channels, nonlinear walk-off attenuates the XPM components due to high-frequency intensity fluctuations, making beats >10 GHz insignificant [17], [18]. The frequency dependence of XPM enables compensation using only low-bandwidth components, and is emulated with a low-pass filter (LPF) [13]. Further, as the low-frequency XPM components of adjacent WDM channels are similar, the TID-PM shown in Fig. 1 can partially compensate XPM for several WDM channels simultaneously [13], [15], [19]; compensation of eight WDM channels at once was demonstrated in [19]. We previously showed, in simulation, that TID-PMs effectively suppress nonlinearity when used on a span-by-span basis in long-haul WDM systems, both with and without in-line dispersion compensation [15], and for polarization-multiplexed signals [19]. A similar technique using a receiver-side digital phase rotation in place of a PM was demonstrated in [20].

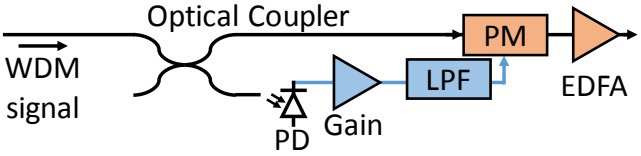


Fig. 1. TID-PM block diagram. PM: Phase modulator; PD: Photodiode; LPF: Electrical low-pass filter; EDFA: Erbium-doped fiber amplifier.

In this paper, we provide the first experimental confirmation that XPM can be mitigated using low-bandwidth opto-electronics. We first transmit two WDM channels with 50-GHz spacing, a 10-Gbit/s on-off-keyed (OOK) interferer and a continuous wave (CW) tone, through an 80-km span of fiber, and show that a TID-PM suppresses the phase distortion on the CW tone caused by the intensity fluctuations of the OOK interferer. We then replace the CW tone with a 28-Gbaud quadrature phase-shift keyed (QPSK) signal, and measure the bit error rate (BER) of the QPSK channel, with and without the TID-PM, as the OOK power is increased. We find that using the TID-PM doubles the allowable interferer power before the QPSK channel to reaches a typical 7% hard-decision forward error correction (FEC) threshold (BER $= 3.8 \times 10^{-3}$). This study shows that low-bandwidth analogue opto-electronics are a feasible way to implement in-line NLC, which may help overcome the nonlinear limits to data rate in optical networks.

Manuscript received November 4, 2016. This work is supported under the Australian Research Council's Laureate Fellowship scheme (FL130100041) and CUDOS – ARC Centre of Excellence for Ultrahigh bandwidth Devices for Optical Systems (CE110001018).

B. Foo, B. Corcoran and A. Lowery are with the Electro-Photonics Laboratory, Department of Electrical and Computer Systems Engineering, Monash University, Wellington Rd. Clayton, Australia 3800 e-mails: (benjamin.foo@monash.edu, bill.corcoran@monash.edu, arthur.lowery@monash.edu).

B. Corcoran and A. Lowery are also with the Centre for Ultrahigh bandwidth Devices for Optical Systems (CUDOS), Australia.

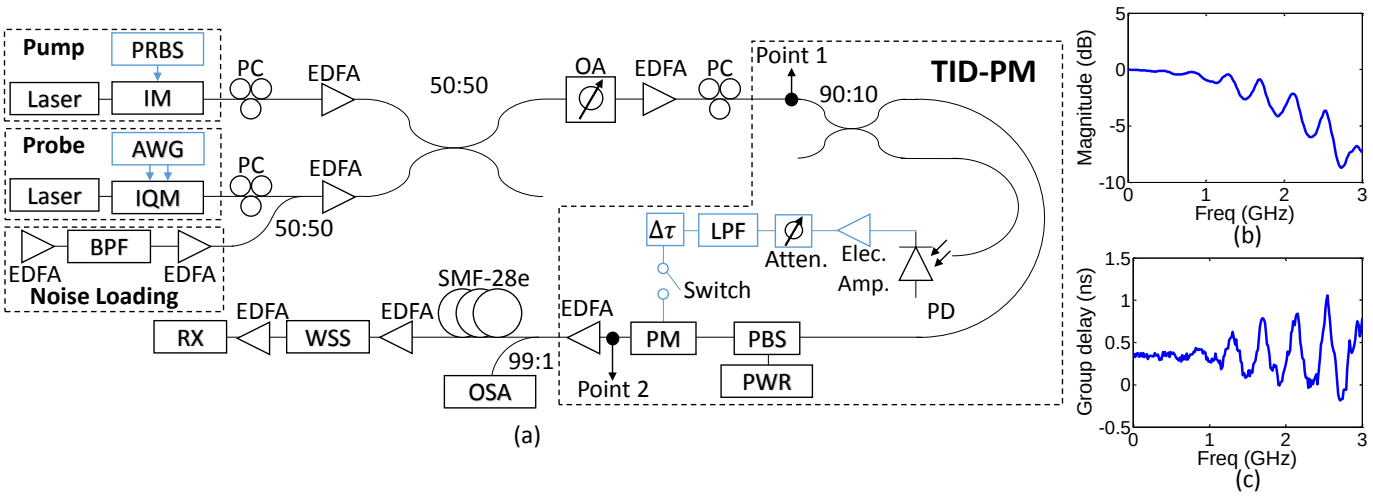


Fig. 2. (a) Experimental pump-probe setup. A 10-Gbit/s OOK pump is transmitted together with a probe, either a CW tone (IQM and noise loading not used) or a noise-loaded single-polarization 28-Gbaud QPSK signal, through an 80-km span of fiber. PRBS: Pseudo-random bit sequence pattern generator; IM: 10-Gbit/s intensity modulator; PC: polarization controller; IQM: 35-GHz bandwidth IQ modulator; AWG: Arbitrary waveform generator; BPF: Bandpass filter; OA: Optical attenuator; PD: Photodiode; Elec. Amp.: Electrical amplifier; $\delta\tau$: Variable electrical delay; LPF: Electrical low-pass filter; Atten: Electrical attenuator; PBS: Polarization beam splitter; PWR: Power meter; PM: Phase Modulator; WSS: Wavelength selective-switch; RX: Coherent receiver. (b) LPF frequency response; (c) LPF group delay.

## II. Experimental Setup

Figure 2(a) shows the experimental setup. Two tunable external cavity lasers, with <100 kHz linewidth, were used to generate the pump and probe signals with 50-GHz separation. Initially, a CW tone was used as the probe, while the pump was a 10-Gbit/s OOK signal. The pump data was a pseudo-random bit sequence of length $2^{31}-1$, and was modulated onto a laser with a 10-Gbit/s intensity modulator. The CW tone was later replaced with a 28-Gbaud QPSK channel, generated by driving a 35-GHz electro-optical bandwidth IQ modulator with a 90 GSa/s arbitrary waveform generator (AWG). In this case, the data on the OOK pump was also stored in the AWG before driving the intensity modulator; the two independent bit sequences were generated in MATLAB and up-sampled to match the sample rate of the AWG. This combination of OOK and QPSK channels might be found when upgrading a legacy 10-Gbit/s link with 100 Gbit/s channels. To enable accurate BER estimation for the short link length, noise was added to the QPSK channel to achieve an optical signal-to-noise ratio (OSNR) of 9 dB, measured on an optical spectrum analyzer (OSA) using a 0.1-nm noise bandwidth. Data was only modulated onto a single polarization for all channels, and polarization controllers were used to co-polarize the two channels. Two erbium doped fiber amplifiers (EDFAs) were used to control the power ratio of the pump and probe, and another EDFA controlled the total power into the TID-PM.

The TID-PM was placed before the span to accurately estimate the waveform along the effective nonlinear length of the fiber (i.e. in the first 20km). A 10-GHz bandwidth photodiode measured the power from the 10% arm of a 10:90 coupler, and an electrical amplifier with fixed gain was combined with a variable attenuator to boost the signal. An off-the-shelf Mini-Circuits SBLP-1870+ was used to emulate nonlinear walk-off. The frequency response and group delay of this LPF, measured using a 3-GHz bandwidth vector network analyzer, are given in Figs. 2(b) and (c), respectively. A variable delay line was used to path match the optical and electrical arms so that the signals entering the PM were properly aligned, and a switch connecting the electrical path to the PM was used to enable and disable NLC. However, the TID-PM was not removed from the system and so still caused a 9-dB loss, measured between Point 1 and Point 2 in Fig. 2(a), when NLC was disabled. As the PM is polarization-sensitive, a polarization beam splitter (PBS) and polarization controller are used to that ensure the signal enters the PM at the correct polarization. This is unnecessary if a polarization-insensitive PM is used [19]. The output EDFA amplified the signal to match the level at the TID-PM input before launching the signal into the link.

The link was one 80-km span of SMF-28e (ITU-T G.652.D standard). After the span, a liquid-crystal-on-silicon wavelength selective switch provided a 40-GHz bandwidth filter to de-multiplex the probe signal. The probe was then pre-amplified and received on a 25-GHz bandwidth coherent receiver using a local oscillator with <100 kHz linewidth. The electrical output from the receiver was stored in a 40-GSa/s real-time sampling oscilloscope for offline processing.

## III. Results

### A. CW Probe

The phase of the CW probe was measured to demonstrate that a TID-PM can suppress the phase distortion due to intensity fluctuations of the OOK interferer. After frequency offset compensation, the phase of the CW tone was reconstructed using in-phase and quadrature components. A 100-MHz bandwidth high-pass filter was used to remove low-frequency phase noise so that only the contributions to phase noise from XPM were measured. The spectral components of the phase waveform were obtained via the Fourier transform, the magnitude of which gives the phase noise spectrum.

Figure 3 plots the phase noise spectra, averaged over 10 measurements, of the CW tone with (dashed blue line) and without (solid red line) the TID-PM at different launch powers into the link. The phase spectrum when only the CW laser is

transmitted, i.e. the residual laser phase noise after high-pass filtering, is also plotted for reference (dotted green line). Traces are plotted with a frequency resolution of 50 MHz for clarity.

With a total launch power of 0 dBm (Fig. 3(a)), XPM is negligible and all three traces are similar. When the power is increased to 5 dBm (Fig. 3(b)), the XPM on the CW tone becomes noticeable. However, this small phase distortion is almost completely suppressed by the TID-PM. At 10-dBm launch power (Fig. 3(c)), XPM causes a relatively large phase distortion. While the TID-PM is unable to fully mitigate XPM, the phase distortion is still significantly reduced. This shows that the TID-PM can effectively mitigate the phase distortion due to XPM from the adjacent OOK signal. The reduced phase distortion should result in a better BER when a TID-PM is used on a data-carrying channel.

### *B. 28-Gbaud QPSK Probe*

We replaced the CW tone with a QPSK signal to ascertain if the phase noise suppression shown in Fig. 3 reduces the BER of a data-carrying channel. In this case, the QPSK channel was launched into the link at 0 dBm, and the OOK power was varied between 0 and 17 dBm. This was achieved by varying the power ratio between the channels, and measuring the power into the link with an OSA. MATLAB processing involved frequency offset and phase noise compensation, followed by frequency-domain chromatic dispersion compensation using the overlap-add method. The signal was equalized with a 21-tap dynamic equalizer using the least-mean-squared algorithm before the BER was found by direct error counting.

Figure 4 plots probe BER against OOK interferer power with (blue circles) and without (red diamonds) XPM mitigation from the TID-PM. A reference BER of $3.8 \times 10^{-3}$ is also plotted, corresponding to a typical target BER for 7% hard-decision FEC codes. When the TID-PM is used, the OOK power can be increased by 3 dB, from 11 dBm to 14 dBm, before the FEC threshold is reached. The constellations of the received signal at 14-dBm OOK power are shown in the inset of Fig. 4. The crescent-like distribution of the uncompensated constellation points indicates the presence of phase noise, which can be suppressed by the TID-PM, as evidenced by the circular distribution of the compensated constellation points. Figure 5 plots the XPM penalty to the $Q$ of the probe signal against OOK power for experimental measurements (markers), and simulation results (dashed lines) obtained from VPItransmissionMaker. The simulated fiber was modelled with 0.2 dB/km attenuation, 16 ps.nm$^{-1}$km$^{-1}$ dispersion, and a nonlinearity coefficient of 1.3 W$^{-1}$km$^{-1}$. The responses in Figs. 2 (b) and (c) were imported into the simulation engine to model the LPF. Simulation and experimental results are in good agreement, though the simulation reports a slightly larger penalty in the uncompensated signal. Although polarization was controlled in experiment, it is possible that the two channels were not entirely co-polarized, reducing XPM distortion [4].

## IV. Discussion

While the above results demonstrate that a TID-PM can be used to suppress the phase distortion from XPM, there are

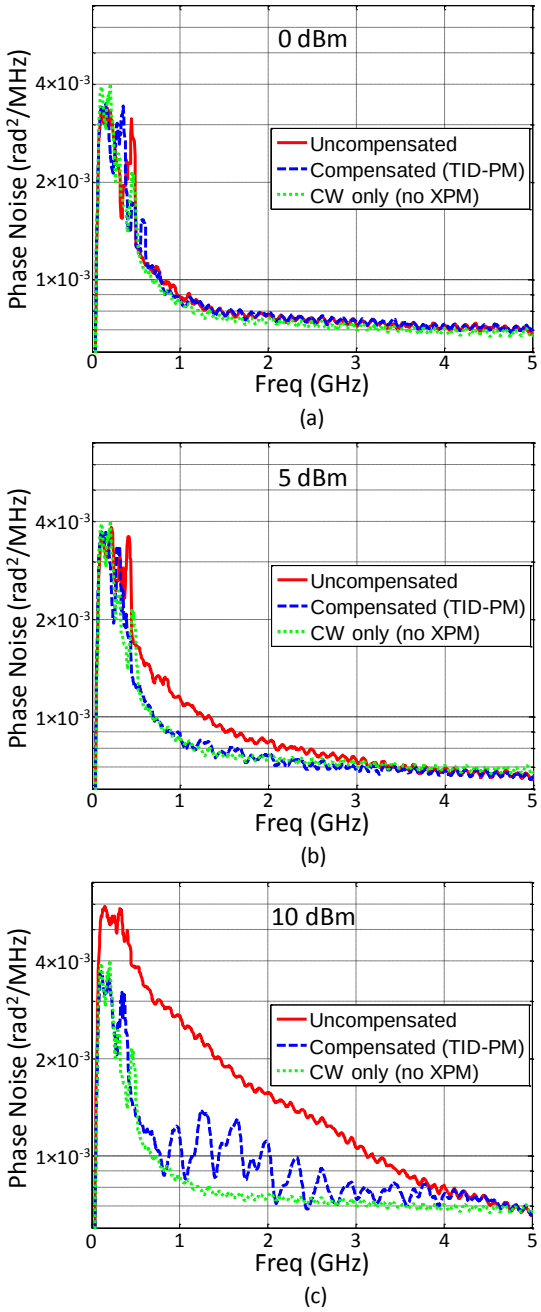


Fig. 3. Phase noise spectral density for the received phase for launch powers of (a) 0 dBm, (b) 5 dBm, (c) 10 dBm, at a frequency resolution of 50 MHz.

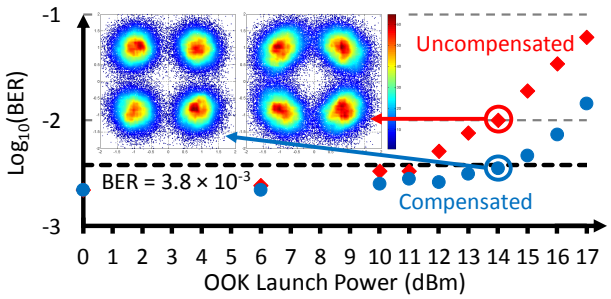


Fig. 4. Pump launch power vs. BER. Inset: Constellations of uncompensated (right) and compensated (left) signals at 14-dBm pump launch power.

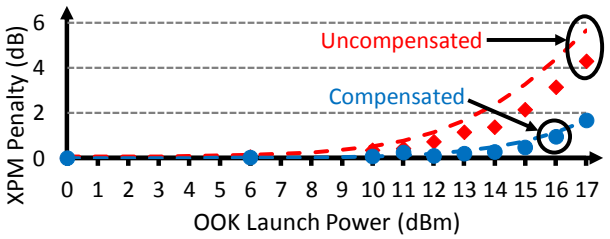


Fig. 5. OOK launch power vs. XPM penalty. Uncompensated: red diamonds; TID-PM compensated: blue circles; Dashed lines: simulation results.

a number of points which must be addressed. First, the off-the-shelf filter used in this experiment was non-ideal, and was chosen because the low-frequency portion (i.e. <2 GHz) of its response was similar to the analytic expression of walk-off from [17]. However, this filter also had large variations in group delay for frequencies above 1 GHz, leading to the ripples observed after XPM compensation in Fig. 3(c). Replacing this filter with one more closely related to the XPM response given in [17] should result in better XPM suppression. However, as TID-PMs are designed to compensate XPM from multiple WDM channels simultaneously [15], the LPF should approximate the walk-off between channels with different frequency separations. Therefore, the filter design that enables optimal NLC remains an open question.

Secondly, the results presented in this investigation do not account for the OSNR penalty caused by the TID-PM; the 'Uncompensated' results were obtained by disconnecting the electrical signal using the switch in Fig. 2(a), but leaving the TID-PM in the link. However, our previous simulations have predicted only a small OSNR penalty when TID-PMs were used in a long-haul link, when the loss of a TID-PM is much less than the loss of a span [19]. It is believed that an insertion loss around 7.5 dB is achievable for a polarization-diverse TID-PM suited for operating in realistic systems [19]; PMs with 2 dB loss can replace the 8-dB loss PM used in this experiment, but elements that add about 4.5 dB of loss are also needed. Additionally, the EDFA at the output of the TID-PM is required to limit its OSNR penalty in a manner similar to the techniques previously used to reduce the impact of using in-line dispersion compensation.

Thirdly, this experiment only considered a simple link as its main objective is to experimentally demonstrate XPM compensation using a TID-PM. Additionally, the OOK signal was launched with higher power than the QPSK channel, which would not occur in a real system. The higher OOK power should be interpreted as an increase in the optimum launch power of a regular system, while the simple link should be viewed as a prototype to demonstrate span-wise NLC. Our previous simulations have shown that in-line TID-PMs can suppress the low-frequency components of the nonlinear distortion on several WDM channels simultaneously [19], are effective in a variety of dispersion maps [15] and can mitigate XPM resulting from OOK [15] and 16-QAM [19] channels, suggesting they are modulation format independent. Additionally, TID-PMs can operate on polarization-multiplexed signals and have potential as in-line NLC in meshed networks [19]. A future demonstration of in-line TID-PMs in a WDM system will endeavour to confirm these predictions.

## V. Conclusion

In conclusion, we experimentally demonstrated a novel NLC technique based on phase modulation using low-bandwidth opto-electronic components. The TID-PM effectively suppressed XPM, thereby improving the BER of an adjacent WDM channel. This proof-of-concept demonstration confirms that XPM can be compensated using low-bandwidth, analogue opto-electronics, providing a new family of devices for increasing data capacity in optical communications systems.

## Acknowledgment

We acknowledge VPIphotonics for support under their universities program.

## References

[1] P. P. Mitra and J. B. Stark, "Nonlinear limits to the information capacity of optical fibre communications," *Nature*, vol. 411, no. 6841, pp. 1027–1030, 2001.
[2] R.-J. Essiambre *et al.*, "Capacity limits of information transport in fiber-optic networks," *Phys. Rev. Lett.*, vol. 101, no. 16, p. 163901, 2008.
[3] A. D. Ellis *et al.*, "Approaching the non-linear Shannon limit," *J. Lightwave Technol.*, vol. 28, no. 4, pp. 423–433, 2010.
[4] G. Agrawal, *Nonlinear Fiber Optics*. Academic Press, 2013.
[5] X. Li *et al.*, "Electronic post-compensation of WDM transmission impairments using coherent detection and digital signal processing," *Opt. Express*, vol. 16, pp. 800–888, 2008.
[6] E. Ip, "Nonlinear compensation using backpropagation for polarization-multiplexed transmission," *J. Lightwave Technol.*, vol. 28, no. 6, pp. 939–951, 2010.
[7] A. Chowdhury *et al.*, "Compensation of intrachannel nonlinearities in 40-Gb/s pseudolinear systems using optical-phase conjugation," *J. Lightwave Technol.*, vol. 23, no. 1, pp. 172–177, 2005.
[8] M. Morshed *et al.*, "Experimental demonstrations of dual polarization CO-OFDM using mid-span spectral inversion for nonlinearity compensation," *Opt. Express*, vol. 22, no. 9, pp. 10 455–10 466, 2014.
[9] E. Temprana *et al.*, "Overcoming Kerr-induced capacity limit in optical fiber transmission," *Science*, vol. 348, no. 6242, p. 1445, 2015.
[10] H. Hu *et al.*, "Fiber nonlinearity compensation of an 8-channel WDM PDM-QPSK signal using multiple phase conjugations," in *2014 Optical Fiber Communications Conf. and Exhibition*, March 2014, pp. 1–3.
[11] A. D. Ellis *et al.*, "Capacity limits of systems employing multiple optical phase conjugators," *Opt. Express*, vol. 23, no. 16, pp. 20 381–20 393, 2015.
[12] K. Solis-Trapala *et al.*, "Nearly-ideal optical phase conjugation based nonlinear compensation system," in *2014 Optical Fiber Communications Conf. and Exhibition*, March 2014, pp. 1–3.
[13] L. B. Du and A. J. Lowery, "Practical XPM compensation method for coherent optical OFDM systems," *IEEE Photon. Technol. Lett.*, vol. 22, no. 5, pp. 320–322, 2010.
[14] L. Du and A. Lowery, "Compensating XPM for 100 Gbit/s coherent channels with 10 Gbit/s direct-detection NRZ neighbors," in *2010 Optical Fiber Communications Conf. and Exhibition*, March 2010, pp. 1–3.
[15] B. Foo *et al.*, "Optoelectronic method for inline compensation of XPM in long-haul optical links," *Opt. Express*, vol. 23, no. 2, pp. 859–872, 2015.
[16] C. Xu and X. Liu, "Postnonlinearity compensation with data-driven phase modulators in phase-shift keying transmission," *Opt. Lett.*, vol. 27, no. 18, pp. 1619–1621, 2002.
[17] T.-K. Chiang *et al.*, "Cross-phase modulation in fiber links with multiple optical amplifiers and dispersion compensators," *J. Lightwave Technol.*, vol. 14, no. 3, pp. 249–260, 1996.
[18] L. B. Du and A. J. Lowery, "Improved nonlinearity precompensation for long-haul high-data-rate transmission using coherent optical OFDM," *Opt. Express*, vol. 16, no. 24, 2008.
[19] B. Foo *et al.*, "Distributed nonlinearity compensation of dual-polarization signals using optoelectronics," *IEEE Photon. Technol. Lett.*, vol. 28, no. 20, pp. 2141–2144, 2016.
[20] L. Du and A. Lowery, "Experimental demonstration of XPM compensation for CO-OFDM systems with periodic dispersion maps," in *2011 Optical Fiber Communications Conf. and Exhibition*, March 2011, pp. 1–3.